Supplementary Information

Online analysis and of single cyanobacteria and algae cells and *Chlamydomonas Reinhardtii* cells under nitrogen-limitation using Aerosol Time-of-Flight Mass Spectrometry

John F. Cahill[1], Thomas K. Darlington[2], Christine Fizgerald[2], Nathan Shoepp[3], Joris Beld[3], Mike Burkhart[3], Kimberly A. Prather[3,4]

[1]*Oak Ridge National Laboratory, Organic and Biological Mass Spectrometry group, Oak Ridge, Tennessee, 37932*
[2]*nanoComposix, San Diego, California, 92111*
[3]*Department of Chemistry and Biochemistry, University of California, La Jolla, California, 92093*
[4]*Scripps Institution of Oceanography, University of California, La Jolla, California, 92093*

*corresponding author e-mail: kprather@ucsd.edu, 858-822-5312, Fax: 858-534-7042

Data filtering method to segregate whole cells from cell fragments for nutrient deprivation experiments

As *Cr* cells undergo starvation their cell wall weakens causing increased fragmentation due to the high vacuum in the SCMS; however, distributions of whole cells still exist and are measured. Size distributions alone, with reference to APS measured distributions, are adequate to segregate whole cells from cell fragments when the extremes of starvation has been reached (i.e. day 4). For days 2-3 size distributions are not enough to confidently remove the cell fragment population from the dataset as the whole cell and cell fragment size distributions overlap significantly.

To isolate whole cells from cell fragments size distributions in combination with mass spectral peak height distributions are used. Since the SQDG lipid at *m/z* -794 is primarily discussed in this manuscript, its peak height distribution is used to isolate whole cells. Figure S-1 shows an exemplary combined size and peak height distribution for starved *Cr* cells from trial 1

on day 4. It can be seen in Figure S-1 that the two modes of the SCMS size distribution are more clearly defined when the peak height dimension is added. The cutoff for isolating the whole cell distribution is given by the red trace in Figure S-1. The uncorrected and corrected APS and SCMS size distributions for the same day can be found in Figure S-2. The SCMS size distribution agreement with the APS measured size distribution improves dramatically after filtering. The filtering size and peak height cutoff was manually determined for each day of the trial. For normal growth samples and day 1 of nitrogen starved samples where there was no evidence of cell fragmentation, the cutoff was simply set to >2 μm to remove small particle noise.

Cell Preparation

5 mL cultures in 15 mL Falcon tubes were started from plates by scraping a portion of the plate and re-suspending in 1 mL of media before addition to the tube. High salt medium (HSM)[1] was used for the scale-up of all freshwater species, with the exception of *Asp* which was cultured in a modified HSM media.[2] All media was autoclaved prior to use. All liquid cultures were grown on a rotary shaker at 140 rpm in a CO_2 box under an atmosphere of 1% CO_2, at a temperature of 27.0 ˚C and an irradiance of 80 μmol m^{-2} s^{-1}. To remove excess salt, cells were pelleted and re-suspended twice in MilliQ water before being resuspended in 35% EtOH. Solutions were diluted to contain ~$2x10^6$ cells/mL measured via hemocytometer. Cells were nebulized and passed through a heated flow tube and diffusion dryer. The output is then sent to an aerodynamic particle sizer (APS) and the SCMS in parallel (Figure S-3).

Susceptibility of cells to high vacuum conditions

Whole cells have been shown to exist within the SCMS; however it quickly became apparent that some cells were fragmenting within the instrument. While not ideal, cell fragmentation does not contaminate whole cell signal since the SCMS can differentiate the data based on size. Comparison of detection efficiencies, calculated by dividing SCMS and APS measured number concentrations, between PSLs and *Cr* cells revealed that *Cr* cells had significantly lower transmission than PSLs at 4 μm, ~1% versus 20%, respectively. This is likely due to fragmentation of cells within the high vacuum of the instrument (~10^{-7} Torr); however, many cells are robust enough to survive under high vacuum conditions. In contrast, cultured mammalian cells fragmented extensively resulting in essentially no transmission of intact whole cells to the laser ablation region of the SCMS. The presence of a cell wall in algae and cyanobacteria is postulated to provide structural support so that they remain intact under high vacuum better than mammalian cells. Experimental methods to increase mammalian cell resistance are underway, but high vacuum tolerance of the aerosolized sample is an important prerequisite for SCMS analysis.

Discrepancies between APS and SCMS size distributions was only seen to occur in *Cr* samples after 2 or more days of nitrogen-limited conditions and is likely due to weakening of the cell wall when undergoing nutrient deprivation. Despite this, there is a clear size mode that is due to whole cells in the SCMS data. As further verification that whole cells are transmitted throughout the instrument a particle deposition slide was collected in the particle sizing region (Figure S-4). In this image whole cells are present.

Single cell mass spectra

A brief discussion of the peaks of interest in *Cr* cells (Figure 2) is given here. In the lower mass range (<200 *m/z*), there is evidence of metals ($^{23}Na^+$ and $^{40}Ca^+$) and organic fragment ions ($^{12}C^+$, $^{15}CH_3^+$, $^{59}NC_3H_9^+$) in the positive ion mode. These ions could be present in the cell or were residues from the prepping medium. Additionally, there are unknown peaks between *m/z* 71-122. The dominant feature in the negative ion mode is $^{26}CN^-$, $^{42}CNO^-$, and $^{79}PO^{3-}$ ions. These peaks have been associated with biological material in atmospheric aerosols, namely bacteria.[3] Other peaks in the negative ion mode are inorganic ions ($^{17}OH^-$, $^{35/37}Cl^-$, $^{45}CHOO^-$, $^{50}C_3N/SO^-$, $^{59}CH_3COO/HCNO_2^-$, $^{63}PO_2^-$, and $^{97}HSO_4/HPO_4^-$). Additionally there are unidentified peaks present from *m/z* 106 - 197.

The large mass ions provide some of the more interesting differences. In the positive ion mode, there is a broad range of peaks from *m/z* 143 - 215, 350 - 550, and additional peaks at *m/z* 617, 670, 696, and 720. The cluster peaks between *m/z* 350-550 are separated by *m/z* 14, probably the result of fragmentation from fatty acids.[4] In the negative ion mode, significant peaks were seen out to *m/z* -820. This peak, in addition to a peak at *m/z* -794, has been observed in a single cell mass spectrum of *Cr* collected by Urban et al. 2011. also utilizing laser desorption ionization.[5] The two spectra have many similarities despite differences in technique and laser wavelength (266 vs 532 nm). Urban et al. 2011 assign peaks -793.6 and -819.6 to a phospholipid species based upon TOF/TOF studies and comparison to phospholipid standards. The tandem MS data was not shown for *C. reinhardtii* cells. To specifically identify the peak at *m/z* -794, negative ion electrospray ionization (ESI) tandem mass spectrometry (MS^n) was conducted on nitrogen-limited cells which readily generated the same ion (Figure S-5). Comparison of the ESI-MS^n spectra to literature reports indicate the MS^2 and MS^3 fragmentation profiles are consistent

with ESI mass spectra of the sulfolipid sulfoquinovosyldiacylglycerol (SQDG) structure esterified by two palmitic acids and a palmitic and oleic acid for *m/z* -794 and -820, respectively.[6] The fragment ion at *m/z* -225 was seen in both SCMS and ESI-MS^3 spectra, which is characteristic of the 6-deoxy-6sulfono-hexoxyl residue of a SQDG.[6] As a final verification a SQDG deficient strain of *Cr* cells (CC4153) was analyzed and the peaks at *m/z* -794 and -820 were absent. Additionally the negative ion mode had a broad range of peaks between *m/z* -208 and -301 and -423 and -554. The latter also exhibited a *m/z* 14 fragmentation pattern likely originating from fragmentation of fatty acid chains as observed in the positive ion mode.

Figure S-6 shows the average mass spectrum for each of the cell strains investigated. A detailed discussion of the mass spectrum for each cell type is beyond the scope of this publication; briefly the single cell mass spectra had some similar characteristics to those discussed in section 2.1, namely small *m/z* metal ions and large ions between *m/z* 350-550 with a *m/z* 14 fragmentation pattern. However, there were also many unique spectral characteristics for each cell type, warranting further investigation.

Discussion of the results of nitrogen-limitation over multiple trials

Three separate trials of time-resolved nitrogen-limited measurements were conducted to provide an idea of cell culture variability. Many trends in cell size, growth, and mass spectral ions were consistent across every trial; however for certain features, cell response was found to vary significantly trial to trail and thus each trial necessitates independent characterization.

Growth rates were similar across each trial with nitrogen-replete conditions steadily increasing in cell count and nitrogen-limited conditions remaining stunted in growth. Cell growth for trial 1 is shown in Figure S-7 and is exemplary of each trial. Size distributions from trial 2 and 3 were very similar to trial 1 (Figure S-8). Cells increase in size under nitrogen-limited

conditions while in nitrogen-replete conditions cells remain 4-5 μm in diameter over the entire experiment. SCMS trends in SQDG consistently increase in peak area under nitrogen-limited conditions for every trial. Additionally GC/MS 16:0 fatty acid content was is always higher for the nitrogen-limited condition; however, the daily trend was quite variable.

Mass spectra of *Cr* consistently show an increase in dipalmitic acid SQDG when under nitrogen-limited conditions. Average mass spectra from trial 1 for nitrogen-replete and nitrogen-limited conditions are shown in Figures S-9 and S-10, respectively. The difference mass spectra can be found in Figure 4 of the main text.

Trial 2

Trial 2 was similar to trial 1 with the exception of day 1 for the nitrogen-limited condition which had unusually high SCMS peak area for *m/z* -794 and high 16:0 content by GC/MS (Figure S-11). The trial 2 size distributions for nitrogen-limited conditions are shown in Figure S-8a. Nitrogen-replete size distributions were very similar to those shown in Figure S-8b. In trial 2 cell fragmentation was significantly easier to isolate as the two distributions were more clearly separated in size than that seen in trial 1. APS and SCMS size distributions of the nitrogen-limited sample from the first day already show signs of cell response, as their cell sizes are increased relative to the normal growth reference also taken that day. The only reasonable explanation is that the time between running the samples was enough for the cells to respond to the lack of nutrients. In addition, the color of the cell suspension was noticeably lighter than the normal growth sample indicating a response from the cells to nitrogen-limitation.

With this in mind, it is not surprising that the average peak area of SQDG between nitrogen-limited and nitrogen-replete conditions disagree on day 1 (Figure S-11b). GC/MS 16:0 fatty acid content had an unusual trend relative to trial 1 and 3 as well (Figure S-11a). The

nitrogen limited condition starts at a high value, decreases, and then increases significantly by day 4, while the nitrogen-replete condition decreased steadily day by day. At this time it is unclear why there is such significant deviation between GC/MS data trial by trial. Despite these differences, the SQDG peak area had the same general trend as in trial 1, increasing for nitrogen-limited cells and remaining fixed at lower values for the nitrogen-replete condition (Figure S-11b). Peak area histograms of nitrogen-limited cells shown in Figure S-12 also show the discrepancy already mentioned for day 1 of the trial. Otherwise, the distribution shifts towards higher peak areas over time just like in trial 1. Difference mass spectra between day 4 and day 1 show mostly similar trends to trial 1, except that high mass (>200 *m/z*) ions did not increase over time in the nitrogen-replete condition (Figure S-13).

Trial 3

Trial 3 size distributions show increased sizes for nitrogen-limited conditions as the days of the experiment increased (Figure S-8d) while nitrogen-replete conditions remained the same every day (Figure S-8c). The cell fragment and whole cell distributions are clearly separated, as was the case in trial 2. After data filtering the APS and SCMS size distributions have excellent agreement. The cell growth rate was similar to both trials. GC/MS 16:0 fatty acid peak areas had characteristics of both trial 1 and trial 2 (Figure S-14a). Nitrogen-replete conditions had a decreasing trend with day, similar to trial 2, while for nitrogen-limited cells peak areas increased over time. Average SCMS SQDG peak areas have the same trends seen in trials 1 and 2 (Figure S-14b). Nitrogen-limited cells increase in peak area over time while nitrogen-replete cells remain fixed. SCMS peak area distributions for nitrogen-limited cells are shown in Figure S-15. The distribution shifts towards higher peak areas over time for nitrogen-limited cells just like in trials 1 and 2. Nitrogen-replete conditions have essentially no change in peak area over time.

Difference mass spectra between day 4 and day 1 have mostly similar trends to trial 1 and 2 (Figure S-16). As with trials 1 and 2 the positive change in *m/z* -794 for nitrogen-limited conditions is the most striking feature. Unlike in trials 1 and 2 nitrogen-replete cell fatty acid fragment ions in both the positive and negative ion mode decrease over time. This is consistent with the decrease in 16:0 GC/MS peak area for the nitrogen-replete condition during this trial (Figure S-14a).

References

(1) Sueoka, N. *Proceedings of the National Academy of Sciences* **1960**, *46*, 83-91.
(2) Schoepp, N. G.; Stewart, R. L.; Sun, V.; Quigley, A. J.; Mendola, D.; Mayfield, S. P.; Burkart, M. D. *Bioresource Technology*.
(3) Pratt, K. A.; DeMott, P. J.; French, J. R.; Wang, Z.; Westphal, D. L.; Heymsfield, A. J.; Twohy, C. H.; Prenni, A. J.; Prather, K. A. *Nature Geoscience* **2009**, *2*, 397-400.
(4) McLafferty, F. W.; Tureček, F. *Interpretation of Mass Spectra*; University Science Books, 1993.
(5) Urban, P. L.; Schmid, T.; Amantonico, A.; Zenobi, R. *Anal. Chem.* **2011**, *83*, 1843-1849.
(6) Plouguerné, E.; de Souza, L.; Sassaki, G.; Cavalcanti, J.; Villela Romanos, M.; da Gama, B.; Pereira, R.; Barreto-Bergter, E. *Marine Drugs* **2013**, *11*, 4628-4640.

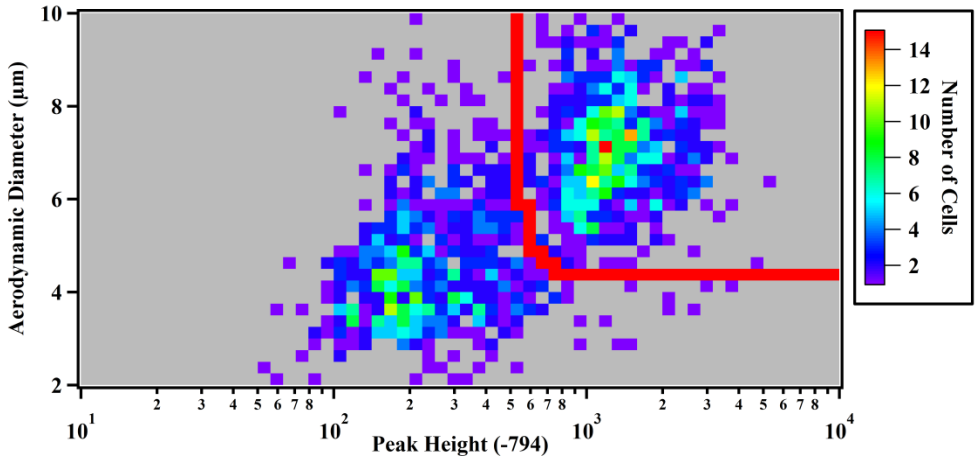

Figure S-1: Exemplary size resolved peak height (-794) histogram of (-N) cells from trial 2, day 4. The threshold values separating cell fragments from whole cells is given by the red trace

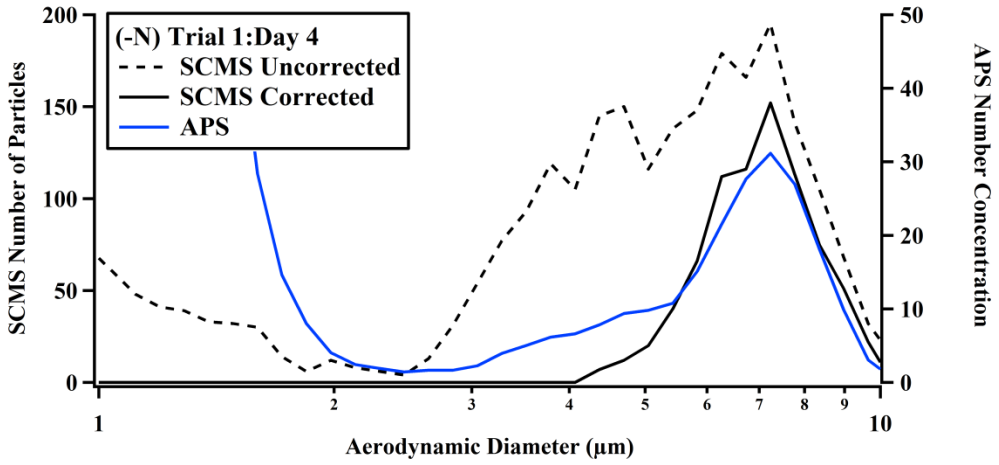

Figure S-2: APS and SCMS size distributions for day 4 of trial 1 for nitrogen-limited cells. The APS trace is in blue, the dashed black line is uncorrected SCMS, and the solid black line is the corrected SCMS size distribution

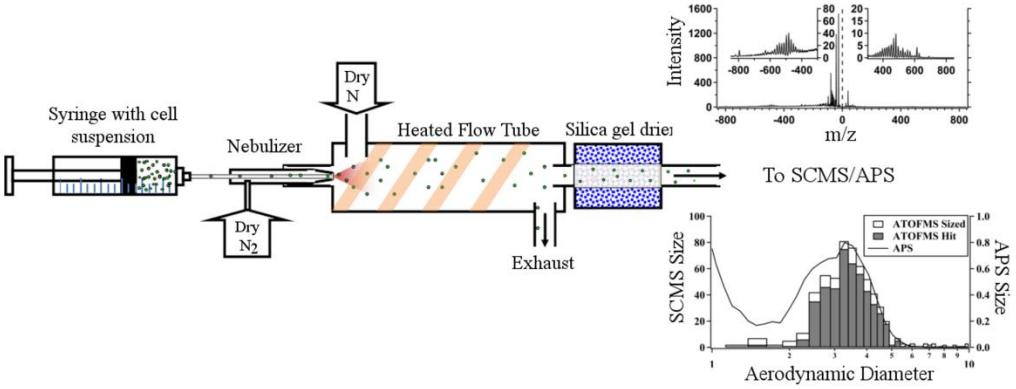

Figure S-3: Nebulization setup for single cell experiments. After drying aerosols are sent to either the APS or SCMS

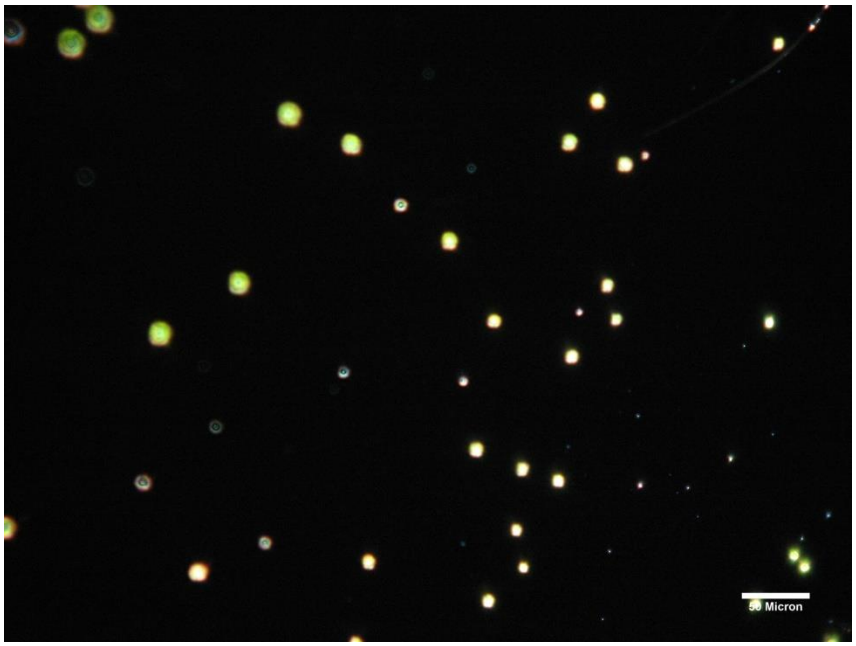

Figure S-4: Green fluorescence images showing whole cells of *Chlamydomonas reinhardtii* collected by deposition within the SCMS

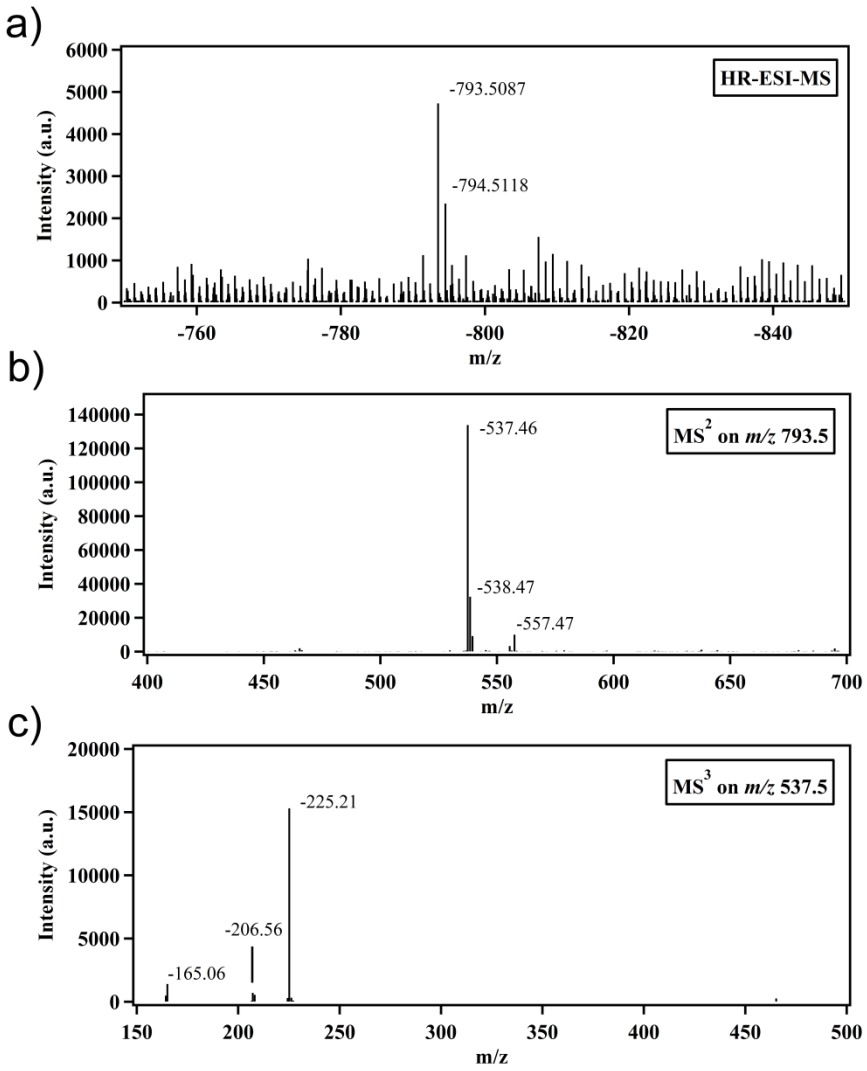

Figure S-5: ESI-MS (a), MS^2 (b), and MS^3 (c) of nitrogen-limited *Cr* cells on day 4

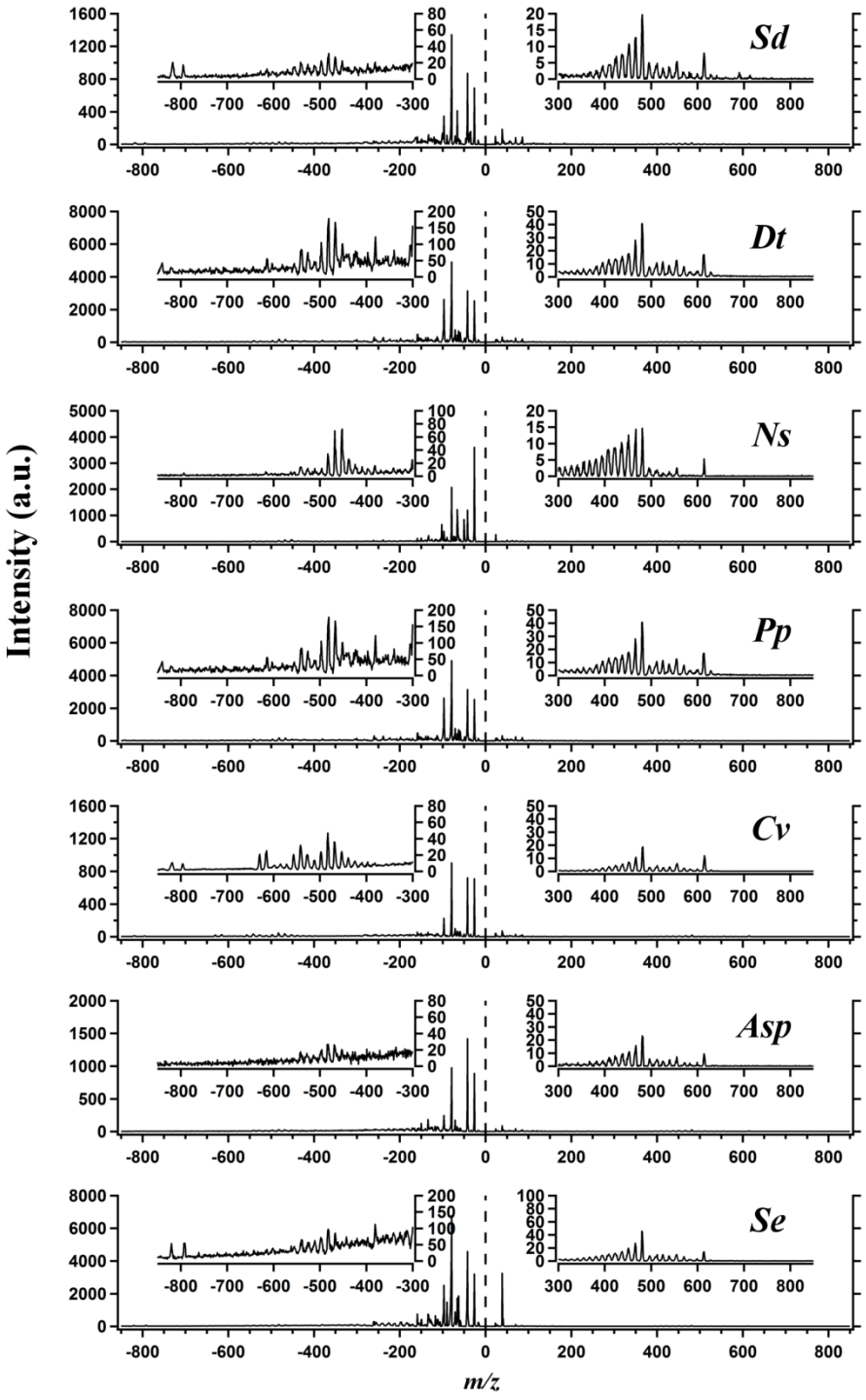

Figure S-6: Average mass spectra of various algae and cyanobacteria cells. Full names of the cells are given in Table 1.1

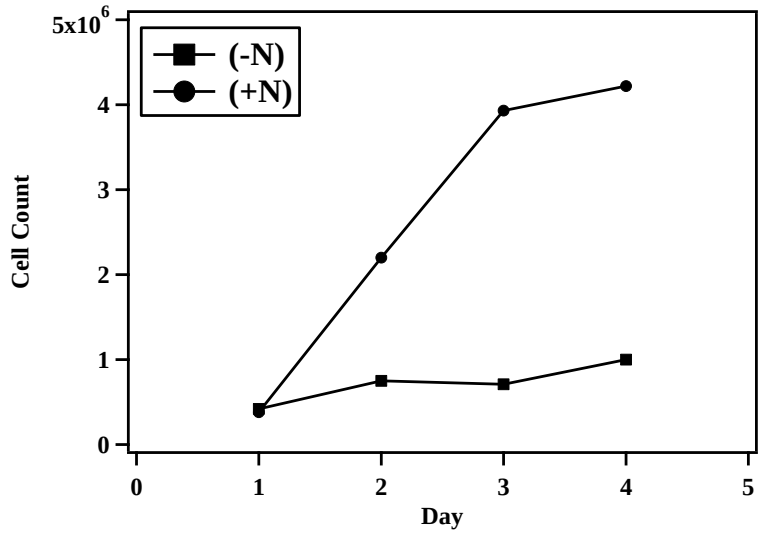

Figure S-7: Cell growth for nitrogen-replete (circles) and nitrogen-limited (squares) conditions for trial 1

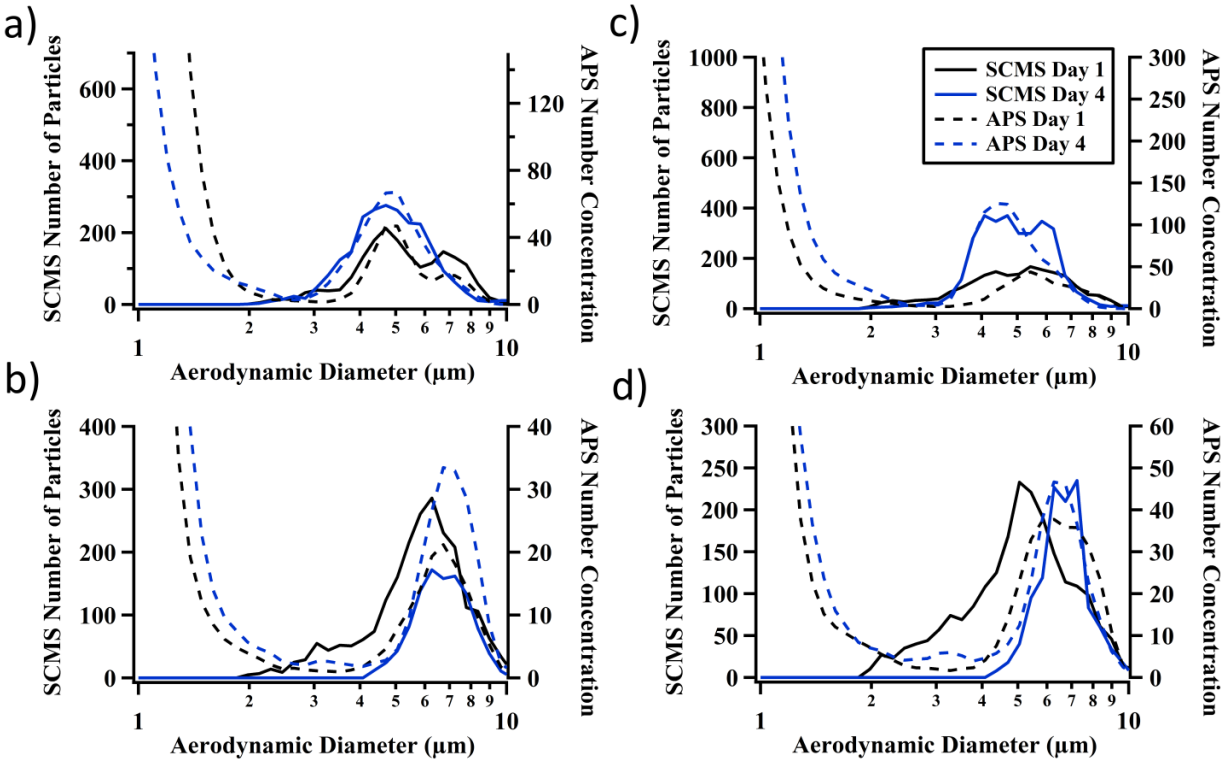

Figure S-8: APS (dashed) and SCMS (solid) size distributions for day 1 (black) and day 4 (blue) under nitrogen-replete (top) and nitrogen-limited (bottom) conditions during trial 2 (a-b) and trial 3 (c-d).

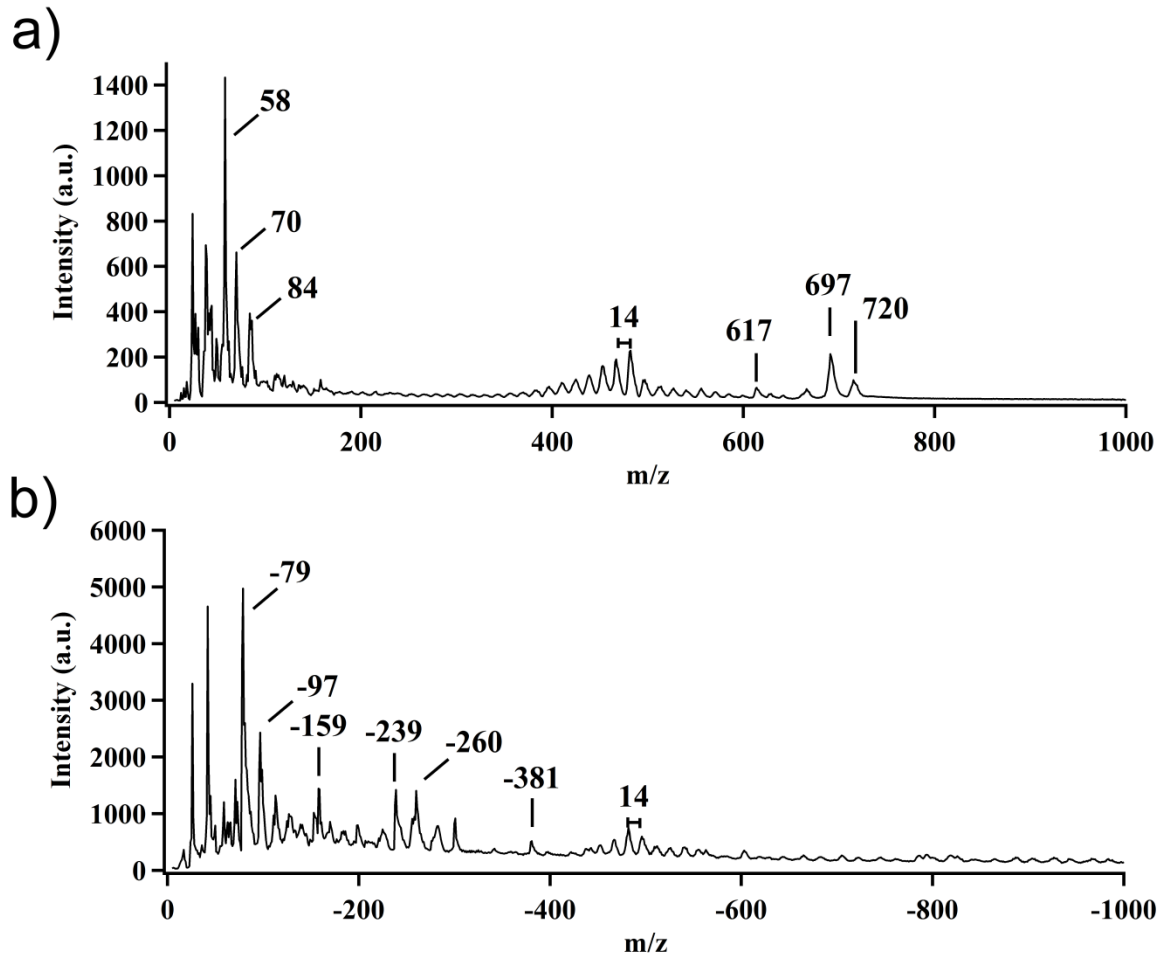

Figure S-9: Positive and negative ion average mass spectra for nitrogen-replete conditions on day 4 of trial 1

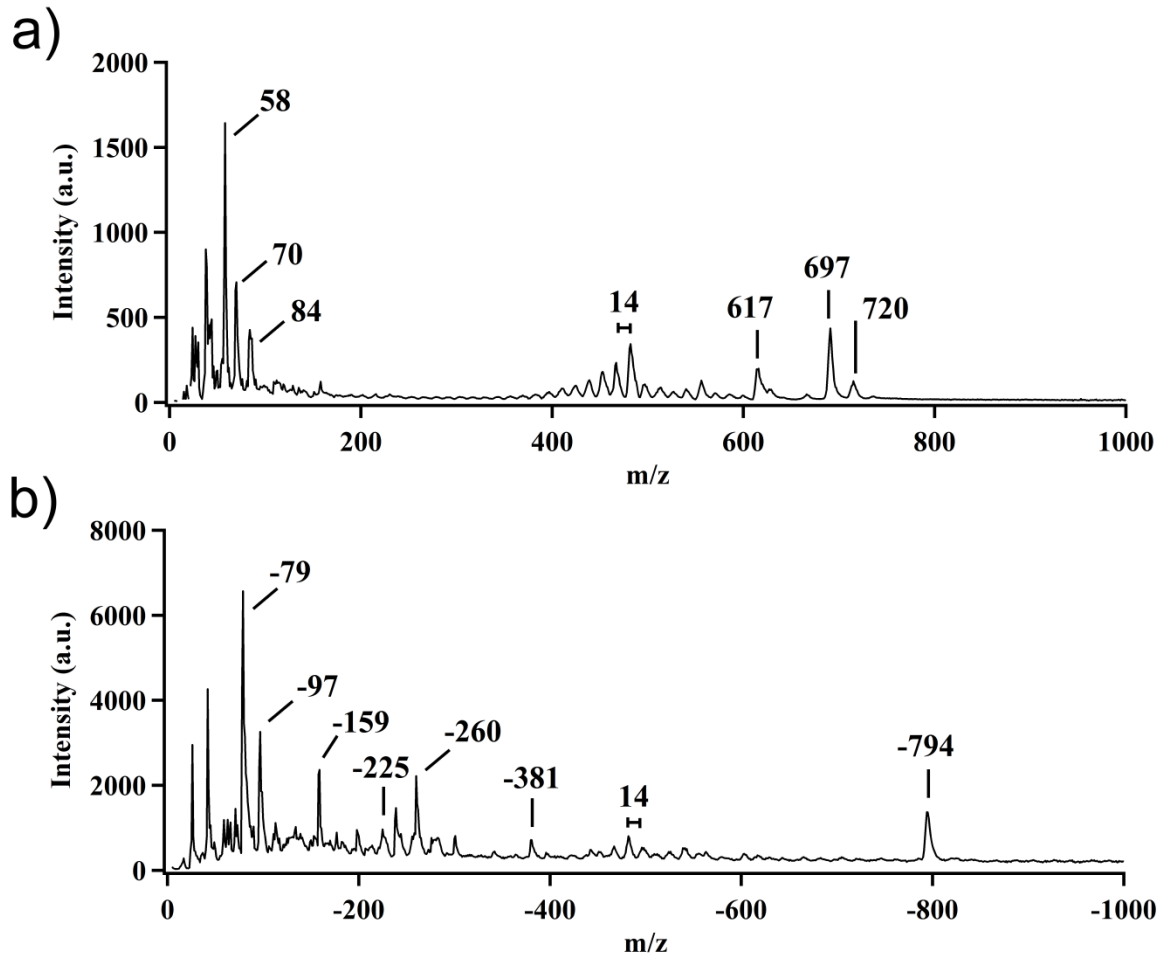

Figure S-10: Positive and negative ion average mass spectra for nitrogen-limited conditions on day 4 of trial 1

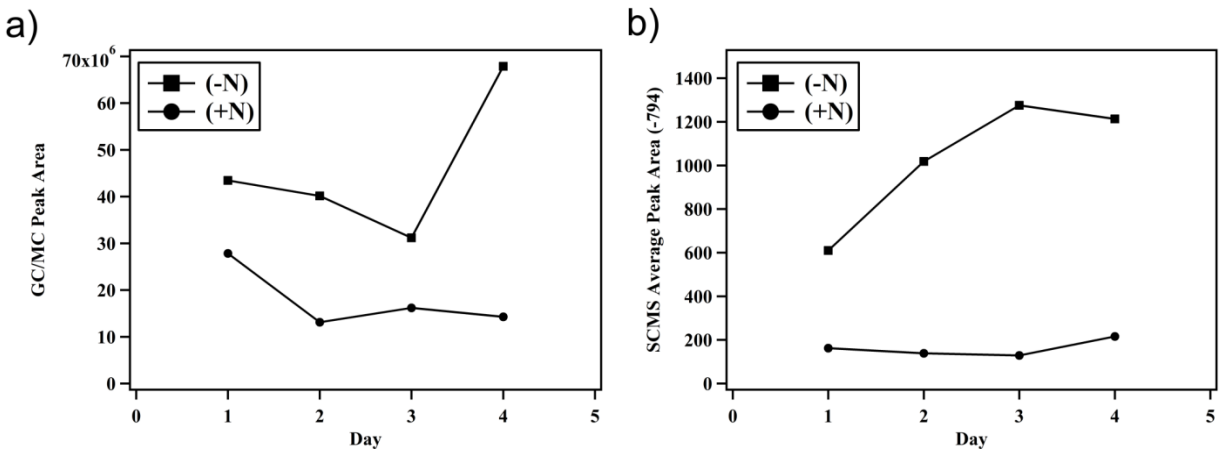

Figure S-11: (a) GC/MS 16:0 fatty acid peak area and (b) SCMS average peak area of -794 for nitrogen-replete (circles) and nitrogen-limited (squares) conditions in trial 2

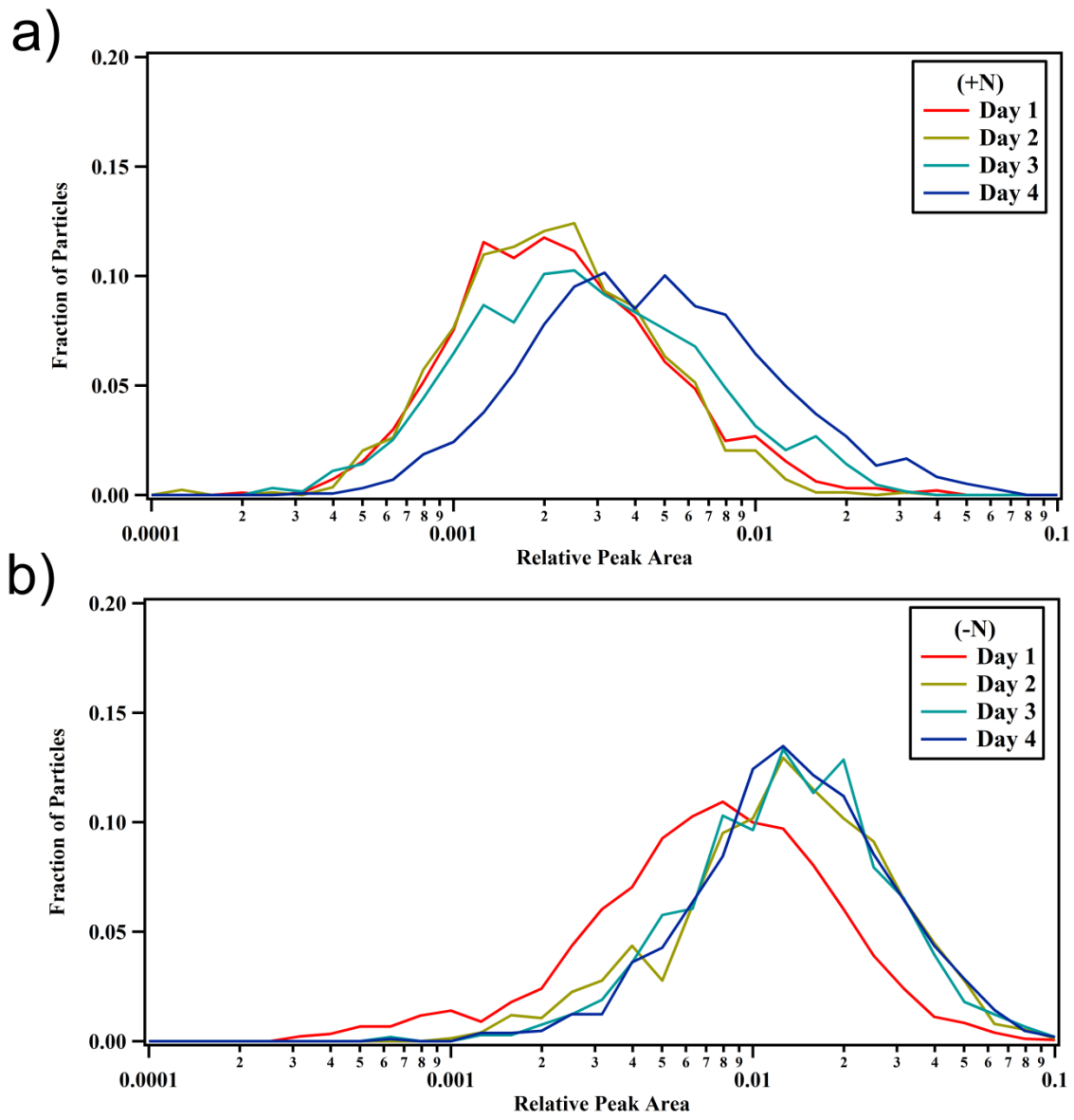

Figure S-12: SCMS peak area distributions for *m/z* -794 under nitrogen-replete (a) and nitrogen-limited (b) conditions for trial 2

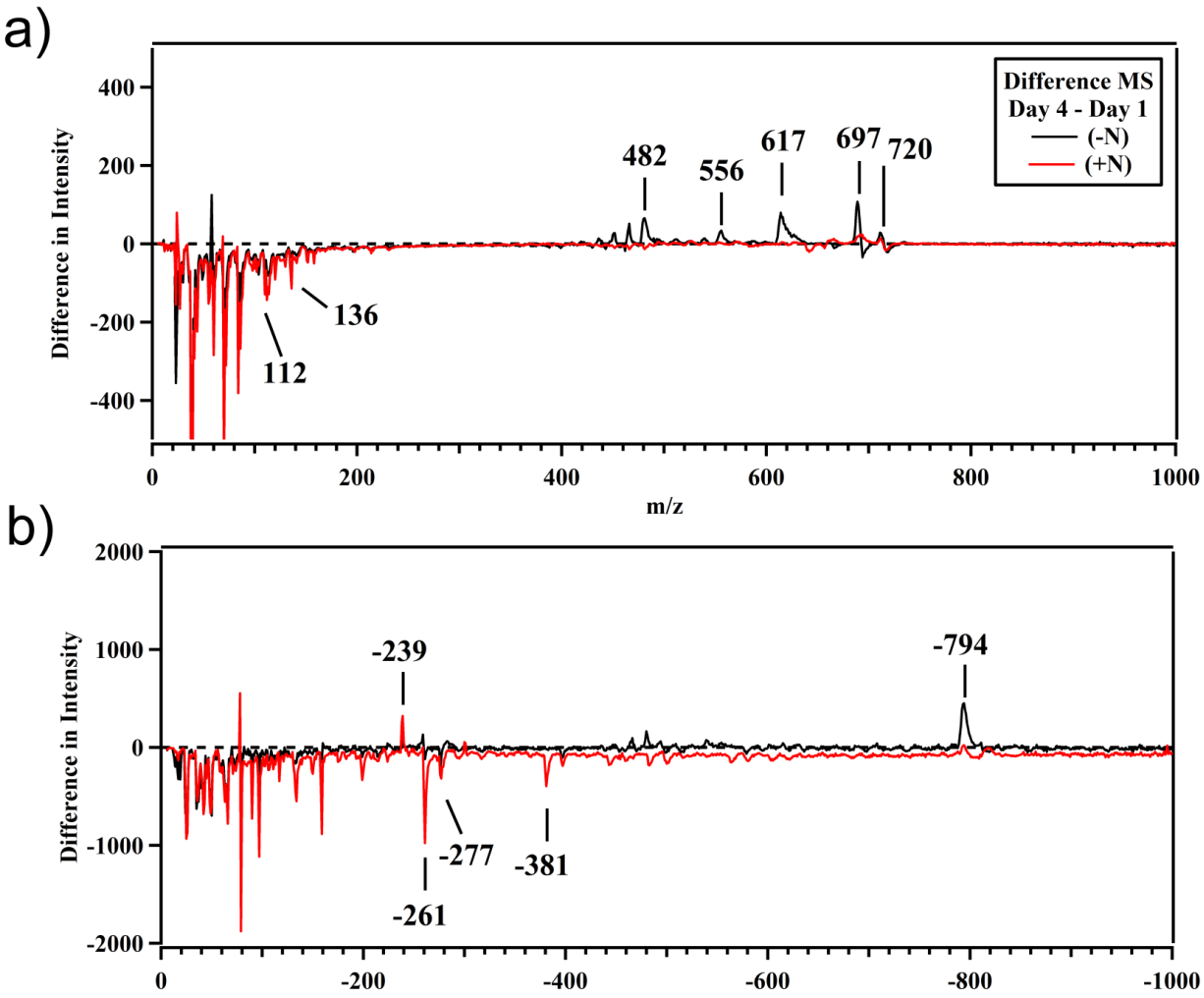

Figure S-13: Positive and negative ion difference mass spectra (Day 4- Day 1) for nitrogen-replete (red) nitrogen-limited conditions (black) in trial 2

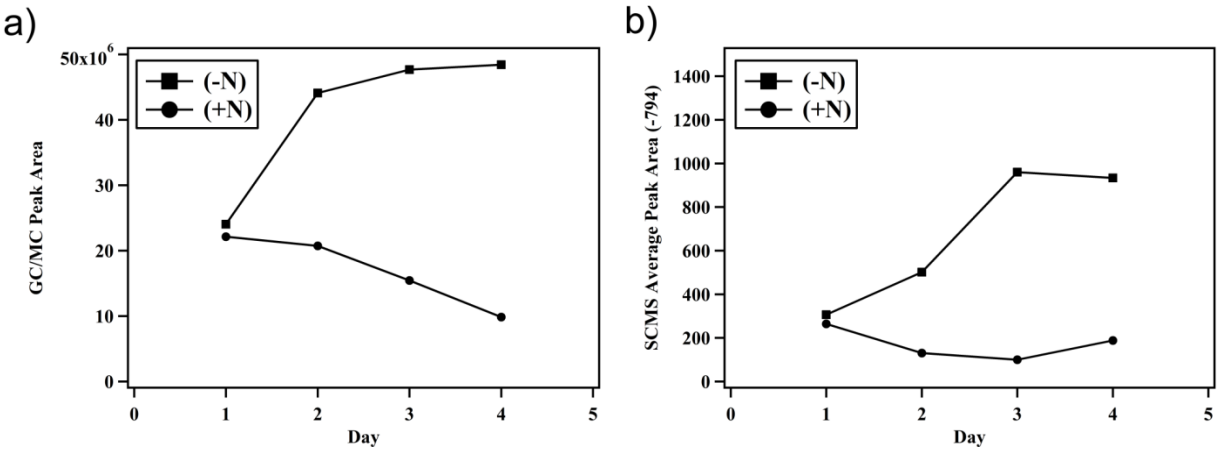

Figure S-14: (a) Ensemble measurement of GC/MS 16:0 fatty acid peak area and (b) SCMS average peak area of -794 for nitrogen-replete (circles) and nitrogen-limited (squares) conditions in trial 3

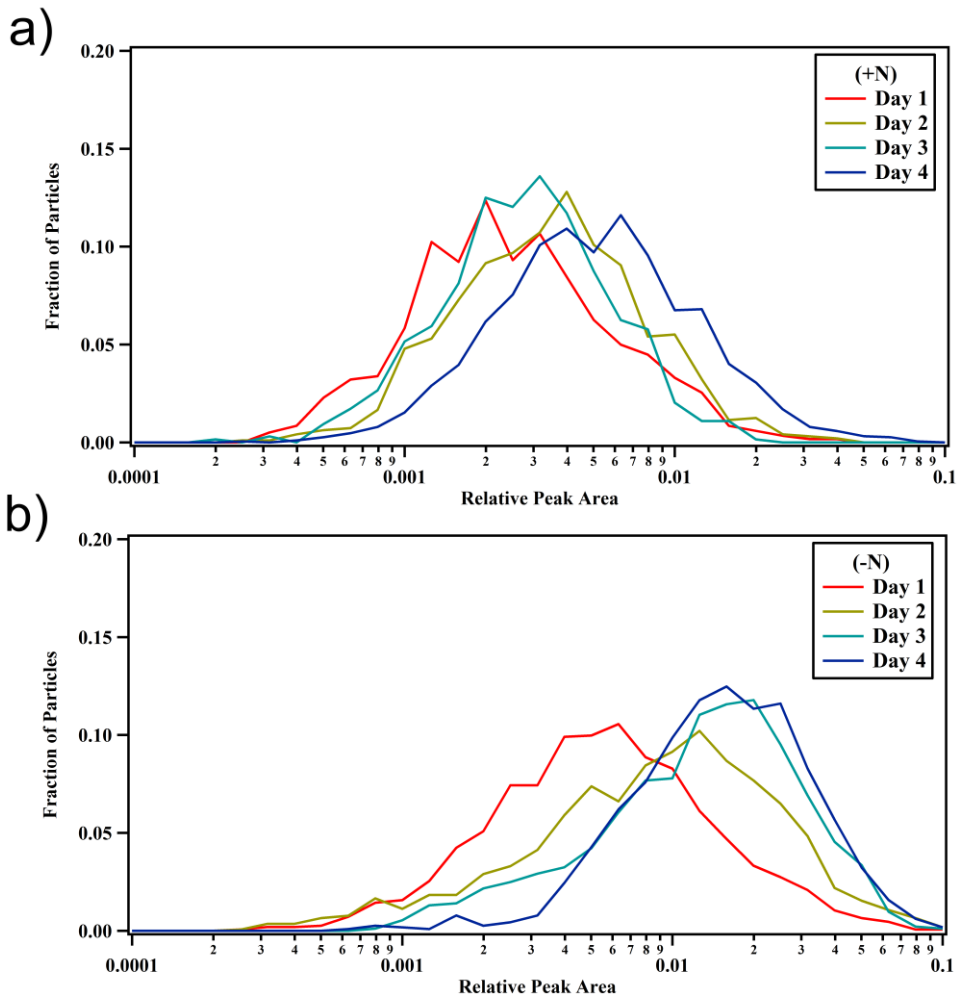

Figure S-15: SCMS peak area distributions for *m/z* -794 under nitrogen-replete (a) and nitrogen-limited (b) conditions

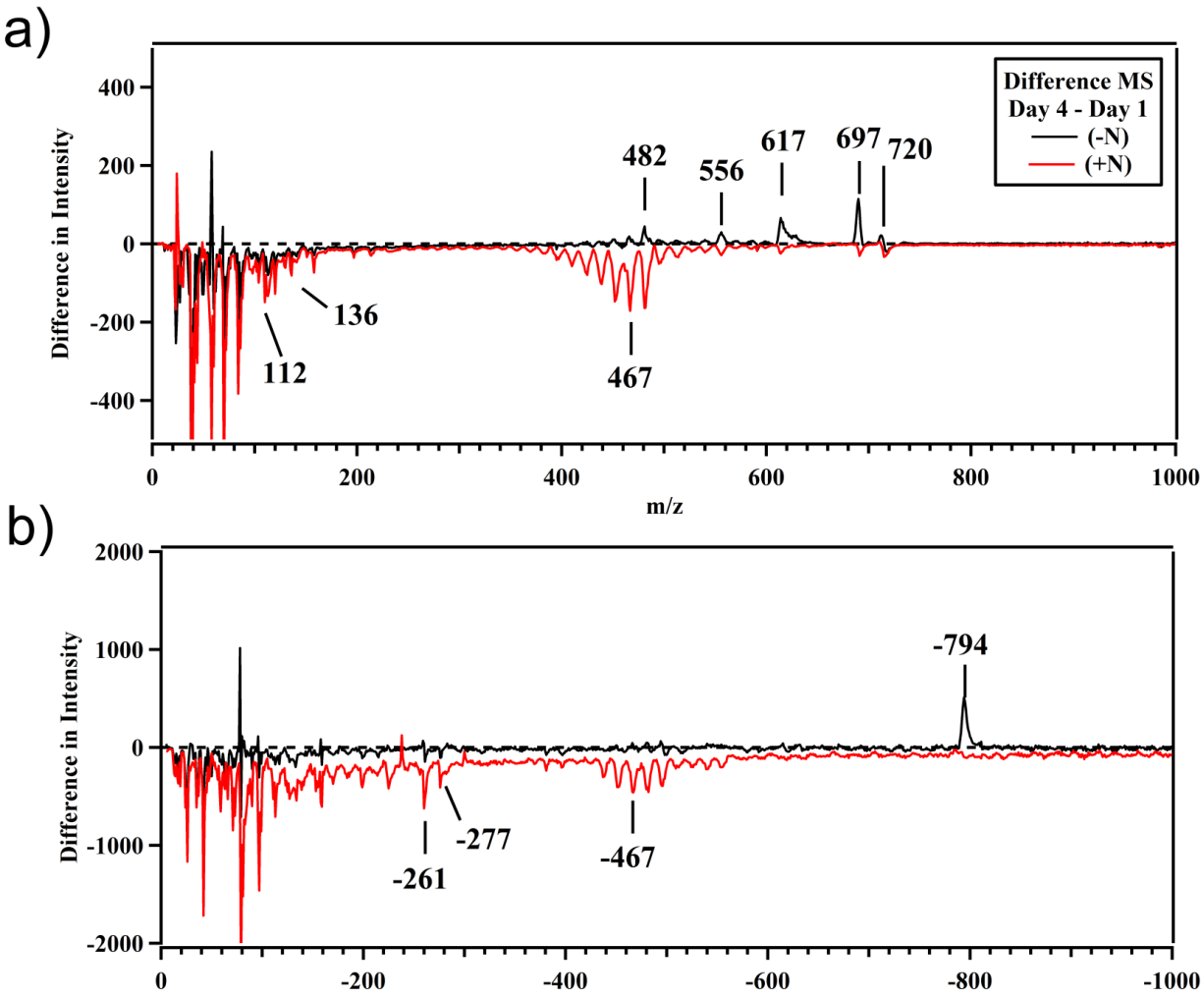

Figure S-16: Positive and negative ion difference mass spectra (Day 4- Day 1) for nitrogen-replete (red) nitrogen-limited conditions (black) in trial 3